NIH Public Access
Author Manuscript
*J Mech Behav Biomed Mater*. Author manuscript; available in PMC 2015 November 01.

Published in final edited form as:
*J Mech Behav Biomed Mater*. 2014 November ; 39: 184–196. doi:10.1016/j.jmbbm.2014.07.015.

# Adaptive properties of human cementum and cementum dentin junction with age

**Andrew T. Jang**[1], **Jeremy D. Lin**[1], **Ryan M. Choi**[1], **Erin M. Choi**[1], **Melanie L. Seto**[1], **Mark I. Ryder**[2], **Stuart A. Gansky**[3], **Donald A. Curtis**[1], and **Sunita P. Ho**[1,*]

[1]Division of Biomaterials and Bioengineering, Department of Preventive and Restorative Dental Sciences, School of Dentistry, UCSF, San Francisco, California, USA

[2]Division of Periodontology, Dept. of Orofacial Sciences, School of Dentistry, UCSF, San Francisco, California, USA

[3]Division of Oral Epidemiology & Dental Public Health, Dept. of Preventive & Restorative Dental Sciences, School of Dentistry, UCSF, San Francisco, California, USA

## Abstract

**Objectives—**The objective of this study was to evaluate age related changes age related changes in physical (structure/mechanical properties) and chemical (elemental/inorganic mineral content) properties of cementum layers interfacing dentin.

**Methods—**Human mandibular molars (N=43) were collected and sorted by age (younger = 19–39, middle = 40–60, older = 61–81 years). The structures of primary and secondary cementum (PC, SC) types were evaluated using light and atomic force microscopy (AFM) techniques. Chemical composition of cementum layers were characterized through gravimetric analysis by estimating ash weight and concentrations of Ca, Mn, and Zn trace elements in the analytes through inductively coupled plasma mass spectroscopy. The hardness of PC and SC was determined using microindentation and site-specific reduced elastic modulus properties were determined using nanoindentation techniques.

**Results—**PC contained fibrous, 1–3 μm wide hygroscopic radial PDL-inserts. SC illustrated PC-like structure adjacent to a multilayered architecture composing of regions that contained mineral dominant lamellae. The width of cementum dentin junction (CDJ) decreased as measured from cementum enamel junction (CEJ) to the tooth apex (49–21μm), and significantly decreased with age (44–23μm; $p<0.05$). The inorganic ratio defined as the ratio of post-burn to pre-burn increased with age within primary cementum (PC) and secondary cementum (SC). Cementum showed an increase in hardness with age (PC (0.40–0.46GPa), SC (0.37–0.43GPa)), while dentin showed a decreasing trend (coronal dentin (0.70–0.72GPa); apical dentin (0.63 – 0.73 GPa)).

© 2014 Elsevier Ltd. All rights reserved.

*Corresponding author at: Sunita. P. Ho, Ph.D., Division of Biomaterials and Bioengineering, Department of Preventive and Restorative Dental Sciences, D2252, 707 Parnassus Avenue, University of California San Francisco, San Francisco, CA 94143, USA. Tel.: + 1 415 514 2818; fax: +1 415 476 0848. sunita.ho@ucsf.edu (S.P. Ho).

**Publisher's Disclaimer:** This is a PDF file of an unedited manuscript that has been accepted for publication. As a service to our customers we are providing this early version of the manuscript. The manuscript will undergo copyediting, typesetting, and review of the resulting proof before it is published in its final citable form. Please note that during the production process errors may be discovered which could affect the content, and all legal disclaimers that apply to the journal pertain.

NIH-PA Author Manuscript
NIH-PA Author Manuscript
NIH-PA Author Manuscript

NIH-PA Author Manuscript

NIH-PA Author Manuscript

NIH-PA Author Manuscript

**Significance—**The observed physicochemical changes are indicative of an increased mineralization of cementum and CDJ over time. Changes in tissue properties of the teeth can alter overall tooth biomechanics, and in turn the entire bone-tooth complex including the periodontal ligament. This study provides baseline information about the changes in physicochemical properties of cementum with age, which can be identified as adaptive in nature.

**Keywords**

Cementum; Age; Dentin; Cementum dentin junction (CDJ); Adaptive properties

## 1. INTRODUCTION

Adaptations to occlusal loads occur within the innervated and vascularized periodontal ligament (PDL), vascularized bone, and cementum (thought to be avascularized) that constitute a bone-PDL-tooth fibrous joint [1]. Overall, the softer PDL and harder cementum, dentin, and bone tissues, including their interfaces, remodel (turnover) in response to a shift in function resulting in a change in matrix properties. When changes in function occur within physiological limits, an adequate PDL-space of 150–380μm is thought to provide an optimum biomechanical function [1, 2]. Optimum function is limited to joints where no significant change in overall displacement of the tooth into the alveolar socket in response to simulated loads is observed [3]. However, inevitable adaptation due to innate age related physiology can manifest as observable differences in tissue properties and their interfaces that makeup the dentoalveolar complex [4]. It is within this context that the physicochemical properties of load bearing cementum tissue will be discussed in this study.

Cementum is a mineralized tissue that covers the outermost layer of a tooth root [5, 6]. The primary function of cementum is to confine tooth motion by way of the PDL, as well as to provide support and load absorption during mastication [6, 7]. In general, cementum exists in two forms, primary and secondary. Primary cementum (PC), which covers the coronal two-thirds of the root is the major contributor for attachment of dentition to alveolar bone [1, 2]. Secondary cementum (SC), which is hypothesized to develop when the tooth assumes occlusion and function, covers the remaining one-third of the root, and is thought to act predominantly as an occlusal load absorber during mastication [2, 8]. While these functional roles are recognized, the time-related implications of changes related to mineralization for PC, SC, and their interfaces with softer PDL are less understood [1, 2]. The physical characteristics of cementum have been previously investigated by identifying its structure, chemical composition, and mechanical properties [9, 10]. Fiber density, calcium-to-phosphate ratio, and hardness of PC have been reported to be different than those of SC [11]. However, studies have only determined the physical properties of cementum at a single point-in-time [9–12], and the interface that it forms with dentin is minimally investigated.

Cementum is not directly fused to dentin. It is attached to dentin via a 100–200 μm thick interface within which a 10–50 μm wide hygroscopic proteoglycan (PG)-rich layer known as the cementum-dentin junction (CDJ) exists [5, 9, 13–17]. Within the CDJ, the dominance of collagen fibers that transverse radially to the mantle dentin are tied with proteoglycans and are thought to contribute to an increased ratio of organic to inorganic content [9, 14]. The

NIH-PA Author Manuscript

NIH-PA Author Manuscript

NIH-PA Author Manuscript

water absorbing fibrous nature of the CDJ may be of importance to transfer loads between adjoining mineralizing tissues implying that, physicochemical changes to the interface could play a key role in the overall biomehanical response to function [9, 13–15]. The collagenous and noncollagenous proteins forming this region exhibit dominant water retention characteristics which have been speculated to help dissipate accumulated function-related stresses [9]. Therefore it is postulated that cementum and its graded interfaces act as biological and mechanical continua allowing for optimum function [10].

Functional demands on a body/organ vary with age and these shifts in mechanical signals can modulate physicochemical properties of tissues [18]. Modulation of physicochemical properties can occur based on the classic tenet that with an increase in age the magnitude of forces on mechanosensitive tissues decrease due to an increase in muscle atrophy [19–26]. Studies specific to the bone-tooth organ have shown an inverse relationship between age and masticatory force, citing decreasing strength of the main masticatory muscles (temporalis, masseter, and medial pterygoid) and muscular atrophy that accompany aging process [23, 27]. It continues to be a challenge to seamlessly tie the cause and effect relationship within the context of functional loads and resulting tissue properties. This is because of the innate feedback between several hierarchical levels, that is, mechanical loads on organs are transmitted and absorbed by tissues which in turn activate cellular mechanisms [24–26, 28] that trigger production of extracellular matrix proteins. Aging and related functional activity have been correlated by measuring changes in bone mineral density, suggesting the lack of daily cyclic loads as a major determinant for tissue atrophy [29]. In fact, cyclic load therapies have been introduced to combat and reverse the bone mineral density loss associated with inactivity, indicating that load is a primary factor to regain and maintain “tissue quality” and overall functional integrity [30]. Hence, in this study, it was hypothesized that the inherent physical and chemical properties of PC and SC change within and across age groups.

The “temporal” and “spatial” response of tissues were investigated by mapping changes in physicochemical properties with age from coronal to apical regions of the root, respectively. Therefore, the objective of the study was to establish spatiotemporal age-related trends in the local structure, chemical composition, and mechanical properties of cementum, dentin, and the cementum-dentin interface.

## 2. MATERIALS AND METHODS

Extracted healthy human mandibular molars (N=43) were collected from adult male subjects according to an approved protocol by the UCSF Committee on Human Research, and were sorted into three groups based on the age of the human subject at the time of extraction (younger=19–39, middle age=40–60, older=61–81 years) [31] (Fig. 1a). The exclusion criterion for tooth samples was periodontal disease which was determined either through patient records and/or through specimen examination post extraction. The teeth were sterilized using 0.31 mrad of γ-radiation [32]. The total sample pool was divided into specimens for chemical and elemental analyses (N=29) (Fig. 1a), and microscopy and indentation (N=14) (Fig. S1).

NIH-PA Author Manuscript

NIH-PA Author Manuscript

NIH-PA Author Manuscript

Single 750 μm thick ground sections were taken from mid region of each tooth (Fig. S1) belonging to the microscopy and indentation group. Each tooth was sectioned by using a diamond wafering blade and a low speed rotary cutter (ISOMET, Buehler Ltd., IL, USA) under wet conditions. The section was subsequently used for CDJ and cementum width analyses. One remaining half of the tooth was embedded in epoxy (Expoxicure, Buehler, Il, USA) for microindentation, while the other half was prepared for structural examination using an atomic force microscope (AFM) and AFM-based nanoindentation technique (Fig. S1).

### 2.1. Light microscopy for cementum and CDJ widths

The 750 μm thick sections were ground and polished to a thickness of 150 μm [9]. The ground specimens with polished surfaces were evaluated for CDJ width and cementum thickness using transmission and reflectance light microscopy techniques (BX 51, Olympus America Inc., San Diego, CA) and Image Pro Plus v6.0 software (Media Cybernetics Inc., Silver Spring, MD) respectively [9]. From the acquired light micrographs, the cementum and CDJ widths were measured using Matlab (Mathworks, Natick, MA). Linear regression was used to determine relationships between normalized root location (NRL), cementum width, and CDJ width (Fig. S1). Statistical significance was determined through analysis of variance (ANOVA) followed by *post hoc* multiple comparison adjusted t-tests (Holm-Šidak, unpaired, two-tails).

### 2.2. AFM and AFM-based nanoindentation for site-specific hardness values and gradients

The remaining longitudinal halves were cut into three or four blocks from the CEJ to the apex (Fig. S1), such that all blocks contained dentin, cementum, and the CDJ (Fig. 3a). The blocks were categorized into either the coronal two-thirds or apical one-third to define the sub-anatomical spatial locations of the tooth. The blocks were then mounted on AFM steel stubs (Ted Pella Inc., Redding, CA) and ultrasectioned as described previously, to generate a relatively flat surface to maintain an orthogonality between the nanoprobes of the AFM and the specimen surface [9]. Qualitative and quantitative analyses of the topography were performed using a contact mode AFM first under dry condition and subsequently scanning under wet conditions (Nanoscope III, Multimode; DI-Veeco Instruments Inc., Santa Barbara, CA), and were analyzed using Nanoscope III version 4.43r8 software (Nanoscope III, Multimode; DI-Veeco Instruments Inc., Santa Barbara, CA) [33].

Wet nanoindentation (N=3 per age group) was performed using a Hysitron Triboindenter (Hysitron Incorporated, Minneapolis, MN). A top-down optics system was used for viewing the specimen surface and selection of testing sites. Specimens were kept hydrated with deionized water throughout testing to mimic conditions closer to *in vivo*. A sharp diamond Berkovich indenter with a radius of curvature less than 100 nm (Triboscope, Hysitron Incorporated, Minneapolis, MN) was fitted to the transducer for elastic modulus and hardness measurements. For each specimen block, three rows of indents with 6 μm between each indent were made in single lines from the cementum enthesis to dentin. Cementum enthesis is defined as the edge representative of the root surface. A maximum load of 1500 μN was used. The loading curve for the nanoindentation cycle consisted of three 4.5 s

NIH-PA Author Manuscript

NIH-PA Author Manuscript

NIH-PA Author Manuscript

segments of load, hold, and unload. Site-specific reduced elastic modulus ($E_r$) and hardness (H) values were evaluated using the Oliver-Pharr method [34].

### 2.3. Inductively coupled plasma mass spectrometry (ICP-MS) for elemental concentration

Another set of transverse sections 2–3 mm thick were cut along the roots of mandibular molars (N=29) using a diamond wafering blade on a low speed rotary cutter (ISOMET, Buehler Ltd., IL, USA) under wet conditions (Fig. 2a). Cementum was isolated from these specimens by removing tubular and mantle dentin using a high speed dental hand-piece (Lares 757 workhorse high-speed hand-piece, Lares Research, Chico, CA) (Fig. 2a). Isolation of cementum was confirmed using a light microscope (BX-51, Olympus America Inc., San Diego, CA) (Fig. 2a).

Cementum specimens were desiccated for 6 months and weighed every 10 days to confirm weight stabilization with the “pre-burn weight” representing the final dry weight before burning the specimens to ash. Inorganic ratio was determined as the post-burn weight of the samples divided by the pre-burn weight. The specimens were then transferred to aluminum oxide crucibles (CoorsTek Inc., Golden, CO) and placed in a furnace (Ney, Bloomsfield, PA) for 24 hours at 1000°F (540 °C) [35]. The ash was cooled to room temperature and a post-burn weight was immediately recorded.

The ash was analyzed for elemental content using the ICP-MS (Agilent Technologies, Santa Clara, CA), with a nitric acid matrix [35]. The technique was used to detect amounts of calcium (Ca), magnesium (Mg), and zinc (Zn). However, phosphorous (P) was not measured due to a limitation in the experimental configuration. Bone ash (NIST SRM – 1400) and trace metals in water (NIST SRM - 1643b) were used as internal standards to verify detection and quantification of elements. Results were generated in parts per billion (ppb) and the percent weights were calculated using the initial known weights. Statistical analysis was performed using ANOVA in combination with *post hoc* t-tests.

### 2.4. Microindentation for hardness evaluation

The remaining sectioned halves were embedded in epoxy and polished as previously described [9]. Microindentation was performed under dry conditions according to the American Standard for Testing Materials (ASTM) standard on polished specimen blocks using a knoop microindenter (Buehler Ltd., Lake Bluff, IL). The spatial interval between indents was 35 μm in accordance with ASTM guidelines. Microindentation was performed at a maximum load of 10 gram-force, and the long diagonal of each indent was immediately measured with a light microscope and Image-Pro data-acquisition software. Rows of microindents were made from cementum through CDJ, to the tubular dentin. Each specimen contained 15 rows from the cementum enamel junction to the root apex. Each row contained a minimum of 10 indents. Knoop hardness values ($H_K$) of respective regions were calculated as described previously [9]. Linear mixed effects regression models were used to fit the hardness data for each of the 3 anatomical locations (cementum, CDJ, dentin) with random tooth specimen effects (to account for within specimen correlation) and cementum, age, and cementum by age interaction (if needed) fixed effects. These results were compared against hardness data obtained via AFM-nanoindentation of similar regions.

NIH-PA Author Manuscript

NIH-PA Author Manuscript

NIH-PA Author Manuscript

# 3. RESULTS

## 3.1 Cementum increased with age while CDJ width decreased with age

Light microscopy of ground sections illustrated a transition region between PC and SC. SC was marked by the presence of identifiable lacunae (Fig. 1b, Fig. S2). As a function of anatomical location, cementum width gradually increased from the CEJ to the apex (Fig. 1c). The thickness of PC increased at a linear rate along the root length, while SC did not illustrate a similar pattern. In general, the relationship between cementum width and anatomical location was linear within PC compared to the trend within SC, indicating differing growth/resorption patterns compared with PC. Due to the anatomical dependency of cementum width on root location, the respective width ranges of PC (5–200 μm) and SC (400 μm-1mm) were high (Fig. 1c, Fig. S2). By clustering measurements closer to the CEJ for PC and closer to the apex for SC, SC width (Fig. 1d, Fig. S2) was always greater than PC width ($p<0.05$). The widths of cementum for both primary and secondary cementum types from the younger group were significantly lower than middle age group. Primary cementum widths in older group were statistically higher than the middle group ($p<0.05$), while SC widths were not statistically significant across age groups (Fig. 1d).

CDJ widths as determined by polarized light microscopy in PC and SC regions were also reported (Fig. 1e). In both PC and SC, CDJ width was found to decrease as a function of age ($p<0.05$). However, no statistical difference was found between PC and SC regions except within the older group. In general, PC formed a wide CDJ with dentin compared with SC in specimens taken from younger individuals, where cementum appeared to be fused with dentin with no apparent CDJ in specimens taken from older individuals (Fig. 1e).

## 3.2 Inorganic ratio of PC and SC increased with age and PC was significantly higher than SC within each age group

The inorganic ratio for PC and SC seemed to increase with age, although no statistical significance between age groups ($p>0.05$) (Fig. 2b) was observed. When comparing PC to SC, the inorganic ratio of PC was significantly higher ($p <0.05$) within each age group.

## 3.3 Elemental composition did not change with age or anatomical location

Elemental weight concentration was determined by normalizing elemental weight (using the ICP-MS measurements) with total sample weight (Fig. 2c). Calcium (Ca), magnesium (Mg), and zinc (Zn) were seen to have the highest contribution. From the tested trace metals, the ranking always adhered to the following trend; Ca>Mg>Zn. However, no statistically significant relationship between elemental composition of PC and SC was found by age or anatomical location (Fig. 2c).

## 3.4 Architecture of primary and secondary cementum types

Ultrasectioned specimens (Fig. 3a) were imaged using a light microscope to provide a macroscale view before AFM was performed. Fig. 3a illustrates the two types of cementum based on the absence and presence of lacunae. These features were used to identify types of cementum [1]. Absence of lacunae is more representative of PC, while the presence of lacunae is representative of SC. PC under AFM revealed a single layer containing a higher

NIH-PA Author Manuscript

NIH-PA Author Manuscript

NIH-PA Author Manuscript

number of hygroscopic principal PDL-fibers running perpendicular to the root surface (Fig. 3b). In contrast, SC was composed of a multilayered lamellar structure. Adjacent to the lamellar structure was also the extrinsic fiber-rich cementum which contained hygroscopic principal fibers as revealed by an AFM (Fig. 3c).

Scans of hydrated specimens in the PC region revealed a dense hygroscopic band in the CDJ region referred to as the fibrous fringe by previous investigators [2]. Under hydrated conditions, SC revealed the presence of a lamellar structure formed by circumferential fibers (Fig. 3c). Additionally, repeating bands within the secondary cementum were observed. Hygroscopic principle PDL fiber inserts were also found in secondary cementum. The width of the hygroscopic CDJ region as measured using a light microscope decreased with an increase in age. Results indicated that the hygroscopic CDJ band lost continuity towards the apical third within older age groups (not shown).

### 3.5 Knoop hardness of PC and SC increased with age

Changes in Knoop hardness with age and distance from root edge were graphed to highlight multifactorial trends between age and anatomical location (Fig. 4a). Within both PC and SC, Knoop hardness gradually increased as cementum transitioned to CDJ and to dentin. The data were averaged within all age groups with their respective ranges in order to highlight the gradual increase from cementum to dentin (Fig. 4b). In addition, average hardness values for PC and SC within one standard deviation are shown in Fig. 4b. On average, a steeper gradient from primary cementum to adjacent dentin was observed compared to a less-steep gradient from secondary cementum to corresponding dentin (Fig. 4b).

Spatiotemporal trends in hardness were as follows: PC was consistently harder than SC within all age groups ($p<0.05$). Also, with an increase in age, the hardness of PC and SC regions increased ($p<0.05$). Both results correlate with increased mineralization observed through chemical analysis. Statistical analysis revealed no interaction effects between age and location in hardness values for cementum and CDJ regions. However, an interaction between age and anatomical location in hardness values existed in dentin (Fig. 5a). The hardness of dentin adjacent to SC decreased with age and diverged from the increasing hardness of dentin adjacent to PC (Fig. 5a).

### 3.6. Nanoindentation revealed higher levels of heterogeneity in elastic modulus and hardness values

Heterogeneity in both $E_r$ and H values existed across all ages and regions as seen from AFM-based nanoindentation under wet conditions (Fig. 5a and b). The range of values was especially higher within the dentin (5b). In general, $E_r$ and H values determined by nanoindentation were higher in bulk cementum compared with its interface with the PDL (enthesis) and dentin (CDJ) regions. The $E_r$ and H values within enthesis and CDJ regions were in a similar range (Fig. 5a). The $E_r$ and H values of PC and SC from the older group were significantly higher than those of the middle and younger groups ($p<0.05$). A higher variability in cementum types, compared to their CDJ and entheses counterparts was also observed. Statistically significant trends were not found between middle and younger groups

NIH-PA Author Manuscript

NIH-PA Author Manuscript

NIH-PA Author Manuscript

for both PC and SC. In the older group, PC was harder than SC ($p<0.05$). The same trend was found within the CDJ ($p<0.05$).

### 3.7. Comparison of microindentation and nanoindentation values

A significant decrease in hardness values from dry to wet conditions provided insights on the dominance of organic matter in cementum types, CDJ, enthesial regions, and dentin which could not be analyzed using a microindenter (Fig. 5). Within cementum, both nanoindentation and microindentation showed a general increase in hardness in both PC and SC with an increase in age. However, microindentation showed that PC was consistently harder than SC, whereas nanoindentation showed no difference between SC and PC in younger and middle groups (only PC was harder than SC in the older groups). Finally, within the microindentation values, CDJ was generally harder than its respective cementum region, while nanoindentation values showed the cementum region being harder than the CDJ.

## 4. DISCUSSION

The objective of this study was to identify a baseline for age-related changes in cementum by evaluating and correlating the 1) structural properties using polarized light microscopy and AFM; 2) chemical properties using IPC-MS; 3) mechanical properties utilizing Knoop hardness microindentation and nanoindentation techniques. Besides age and gender, the individual background for each contributing patient is unknown. It is assumed that this cross-sectional study surveyed a diverse ethnic population from San Francisco Bay Area patients visiting UCSF for dental treatment. It should be noted that the observed structural, chemical composition and site specific mechanical properties will be discussed within the context of the load bearing capacity of cementum tissue as related to the bone-periodontal ligament-cementum complex. Additionally, the insights presented in this discussion from a holistic perspective were possible by using currently available state-of-the-art equipment on cementum.

Cementum is one of the four mineralized load bearing tissues in most mammalian species. Cementum covers enamel in most herbivores, serving as a material to endure occlusal wear [37]. However, in humans, cementum primarily covers all of root dentin and overlaps with enamel forming another unique interface known as the cementum enamel junction (CEJ) [38–40]. Interestingly, it forms a weak interface with enamel [38] but a relatively stronger and hygroscopic interface with root dentin. Despite the proximity of cementum to bone (only 150–300 μm), cementum was reported as a mineralized tissue that does not go through the dynamic modeling/remodeling process as bone and PDL [41, 42]. However, considering that many other ligament-bone interfaces in the skeletal structure, including the opposing PDL-bone interface, are influenced by functional loads [43–46], it was hypothesized that age-related changes occur over time as a result of an adaptation to the dynamic loading that occurs across the dentoalveolar complex. To test this hypothesis, cementum from mandibular molars was characterized using high resolution state-of-the-art equipment. Only molars from males were analyzed to minimize potential effects on cementum due to differences in muscle efficiency and hormones compared with females [47]. Since

NIH-PA Author Manuscript

NIH-PA Author Manuscript

NIH-PA Author Manuscript

functional loads were thought to play a role in age-related changes, molars which undergo the largest magnitude of occlusal loads among all tooth types were used to accurately identify spatiotemporal adaptation in cementum and its interface with root dentin. Furthermore, maxillary bone quality significantly differs from mandibular bone which could influence properties of maxillary teeth [48, 49]. Thus mandibular teeth only were selected. Finally, molars extracted due to periodontal involvement were excluded since periodontal disease influences cementum growth and maintenance [46, 50, 51].

Normal physiologic dynamics for cementum is either appositional growth or resorption. Studies have hypothesized that the mechanism for this appositional growth is attributed to mineralization of the organic matter by the cementoblasts in response to mechanical strain along the PDL-cementum interface [7, 52–56]. In line with previous studies, the increase in cementum width over the age groups in both PC and SC (Fig. 1e) support the model that cementum continuously grows in a systematic fashion layer by layer throughout the life of an individual [12]. However, it was identified that cementum growth is controlled with occlusal loads and absence of load can lead to super eruption due to increased apposition of secondary cementum [57]. Hence, it is conceivable that the rate of secondary cementum apposition can increase as the mammal ages and loses its muscle efficiency due to a decrease in function. Following standardization of measurements, an increased variation in SC cementum width suggested that additional factors unrelated to load could significantly influence SC growth (Fig. 1e). PC width also increased but not at the same rate as SC indicating that the mechanistic process for the growth of these layers as a function of anatomical location could be different. The individual growth rate differences in PC and SC, and mutual dependent growth rate could be due to the dominance of variable mechanical strain as a result of the differences in forms (geometrical shapes) of the coronal and apical complexes. Based on the significant differences between PC and SC, we speculate that these mechanisms after the inception of function play a dominant role in defining the commonly known histological structures of primary and secondary cementum types. As a result, PC contained an abundance of principal fibers which created a network throughout a single mineral layer. In contrast, AFM imaging revealed that SC’s architecture contained a circumferential lamellar patterning with hygroscopic fibers running both radially and circumferentially.

The effect of an environment should also be considered when studying tissues and their intrinsic properties as related to functional development. In an oral environment, changes in exogenous and local endogenous pH and alkalinity are thought to play a role in functionally developing alveolar bone and cementum, despite the differential in growth patterns of cementum and bone. Although not categorized, the mineral content presented in this study could also be from intra- and extra-fibrillar compartments within the organic matrix. However, what is minimally understood is the contribution of ratio of organic to inorganic constituents in each of these compartments toward observed structural and chemical heterogeneities, resulting in the mechanical anisotropy as measured through nanoindentation. Observations including increased or decreased mineral contents are consistently made between the radial fibers, fibers within the lamellae, and interlamellae structures [58]. It is possible that a change in the interspersed higher and lower molecular weight proteoglycans due to a local change in pH can aid in increased and decreased

NIH-PA Author Manuscript

NIH-PA Author Manuscript

NIH-PA Author Manuscript

affinities for ions, and over time contribute toward observed mineral contents. Thus the mineral changes identified by others using microprobe [17] and in this study (Fig. 2c) could be due to commonly discussed factors that include cyclical effect of functional loads, development, and available nutrition during a season – all of which may affect the quality of cementum and the rate at which cementum grows [59]. Results presented in this study corroborate with others [5, 8, 14–16] in that the observed structural bands (Fig. 3c) are manifested by variations in collagen orientation and mineral content, which can directly influence both elemental composition and mechanical properties.

The difference in inorganic content (Fig. 2b and c) seen between younger and middle groups compared to differences between middle and older groups is indicative of a general mineralization process throughout cementum, and is likely regulated through a network of mechanically sensitive cementocytes [60]. The change in mineral content with age can be described as an adaptation to decreased load rates coupled with metabolic activity of cells since older individuals present decreased muscle size and strength compared with younger individuals [23, 61]. Additionally, the effect of functional loads is seen most between the younger and middle age groups. Interestingly, similar effects are also observed in rodents, which are often used as animal models to investigate load and disease-mediated adaptations [62, 63].

Generally accepted percentages of inorganic content among dental hard tissues vary from cementum (50%), bone (60%), dentin (70%), and enamel (95%) [30] (Fig. 2b). The inorganic ratio results were above the expected cementum range and within percent mineral of bone and dentin tissues. While these findings could suggest residual dentin in the cored-out cementum rings, as stated earlier, each specimen was inspected under a light microscope for any remnants of dentin. Using ICP-MS, the inorganic component of specimens contained higher amounts of Ca, Mg, and Zn (Fig. 2c) elements. It is expected that calcium exists in higher amounts as it is a major component of apatite [11, 31]. Additionally, our results (Fig. 2c) are in agreement with others, in which decrease in magnesium levels with an increase in age were reported [32]. Sources of zinc could have been derived from both exogenous and endogenous origins. As an endogenous source, zinc has been shown to exist as a part of the transcription factor osterix (OSX) which is shown to help with osteoblast differentiation [64]. Other studies have cited that hydroxyapatite readily uptakes exogenous forms of zinc and is maximized on the root surface (i.e. cementum regions) with the majority of zinc being deposited within dental tissues prior to eruption [65]. Physiologically, zinc levels within the plasma have also been shown to decrease with age, allowing for less accumulation of zinc within dental mineralized tissues in the elderly [65]. Microbial agents such as zinc-citrate and zinc-chloride are exogenous sources of zinc from toothpastes [66]. In addition, elemental Zn is a temporal stamp of tissue metabolic activity, and is currently hypothesized as a key trace element for remodelling and modeling of matrices [67].

Effects of cementum mineralization over age groups can also be seen across the CDJ. Both PC and SC contained hygroscopic fibers which could be traced through the mineralized tissue with an increased density at the CDJ. Often times, the congregated fibrous bundles are best visualized their hygroscopic activity through wet atomic force microscopy (Fig. 1b and Fig. 3b). Compared with specimens from a younger group, specimens from middle and older

NIH-PA Author Manuscript

NIH-PA Author Manuscript

NIH-PA Author Manuscript

groups had a markedly decreased CDJ thickness (Fig. 1b). Thickness of the CDJ in the apical regions were especially affected in the apical regions of molars as the CDJ could not be discerned using both light and atomic force microscopy techniques (data not shown). These structural changes could be a result of mineral formation across the CDJ over time, which decreases the hygroscopic activity and could provide an appearance of fusion of cementum with dentin [17].

Age-related fluctuations in reinforcement of organic matrices with mineral can contribute to changes in hardness values in cementum and the surrounding regions (Fig. 4 and 5) [2]. These findings correlate with the structure and compositional results pointing in the direction of active biomineralization of cementum occurring throughout the life of an individual (Fig. 4b). The hardness values under dry conditions using a microindenter (which has a sampling size several times higher than that of a nanoindenter [9]) provided distinct differences between PC and SC. However, by sampling with a smaller probe under wet conditions, the heterogeneous nature of the tissue under simulated *in vivo* conditions was identified. The heterogeneity could be due to the probe sampling the predominantly organic Sharpey's fibers within the matrix of both PC and SC types. Despite the two hierarchical levels of measuring tissue mechanical properties, the results do not explain the effect of water compartment as the sampling size increased by 1000 times under dry conditions by using a microindenter. However, it is likely that the effect of the individual constituents to their water binding capacity within the volume fraction of material under an indenter is better represented by the nanoindenter. Therefore, we must emphasize the importance of scale factor, sampled volume fraction, and the testing conditions to produce the most representative and complementary results when characterizing materials. This effect is corroborated by the convergence of hardness values under dry and wet conditions for the older age group with a correlation to increased ratio of inorganic to organic contents. Hence, as mammals age, the increased biomineralization restricts and masks the hygroscopic activity of these fibers, thereby causing the inorganic component of the tissue to dominate, but with decreased elastic recoil even under hydrated conditions. These results (Figs. 4 and 5) are indicative of decreased effect of intrafibrillar water compartment within the composite-like material.

While the aforementioned argument could explain the observed physicochemical differences between PC and SC and with time, it does not provide a cause for increased inorganic content and increased hardness of bulk cementum. In other words, it is likely that the cellular processes that lead to biomineralization at a younger age need not be the same as those that prompt biomineralization at an older age. Hence, it is possible that the size of the crystal, its interaction with the organic matrix, and the texture of the material can all be equal contributors to the measured heterogeneity in elastic modulus and hardness observed within PC and SC. Further age-related studies are necessary to identify the nature of biomineralization and the quality of crystal and its interaction with the organic matrix.

From a functional perspective, structural and mineralization effects have been coupled in finite element analysis (FEA) to understand the internal stresses, that occur within tissues and periodontal space highlighting the apical portion of the root as a prominent region resisting compressive loads [6, 68]. Thus it is conceivable that the observed age-related

NIH-PA Author Manuscript

NIH-PA Author Manuscript

NIH-PA Author Manuscript

changes in mineralization, structure, and material properties related trends seen throughout this study can be load-mediated adaptations which accumulate over an individual's lifespan. However, a fundamental question that remains is "why is the structure of cementum, an outer layer of the root surface, lamellar in its architecture?" Cementum structure is analogous to that of growth rings of a tree and similar to that of osteonal architecture in long bone and alveolar bone. Given these analogous structures, the common denominators amongst these structures are functional loads that prompt architecture conducive to resist hoop strain. Hence, our reasoning to support lamellar circumferential growth is limited to a postulate, in that the outer layers of the organic tissue covering the root surface are subjected to hoop strain and prompts mineralization along the strained fibers similar to the formation of osteons in bone. It is also possible that reduced function causes a decrease in hoop strain and a differential in turnover rate of organic and inorganic matter that in turn can contribute to the measured heterogeneity within cementum. From a functional perspective, the observed age-related increase in mineral concentration, decrease in organic component, and decrease in the width of the CDJ would represent an increased concentration of stresses in both cementum and dentin and decreased tissue recovery in respective tissues. This study provides baseline information about the changes in physicochemical properties of cementum with age, and that these properties can be identified as adaptive properties.

## CONCLUSIONS

The physicochemical properties measured within this study were taken to underline the baseline spatial-temporal behaviors of cementum and we postulate are a result of both agerelated and environmental (epigenetic) influences. The growth of cementum width over age indicates a continuous appositional process throughout all sampled ages, but with an affected quality. Cementum mineralization does not cease with initial formation, but rather continues through older ages resulting in further cementation of the CDJ as well as a gross increase in cementum hardness in older groups. As the age of the subject increases, the intrinsic differences in hardness and mineralization content between primary and secondary cementum decrease due to a convergence in mineralization activity.

Cementum properties which show lower correlation and higher variation within groups such as trace element composition could be influenced by additional non-aging factors such as general health, diet, and nutrition. Other results described in this study that show a higher relationship to age (inorganic content, cementum and CDJ width) could imply a natural tendency which is relatively uninfluenced by these environmental variables. Similar studies could be executed in isolated homogenous populations in order to detect the effect of a significant variant as a function of age.

The current dogma suggests the activation mechanism for mineralizing processes in cementum is cyclic function due to mastication. Therefore, future studies should focus on comparing teeth that undergo different mastication loading vectors (such as incisors or cuspids) to further understand the age-related relationship of mastication loads and cementum quality, but relative to the quality of the alveolar bone to which the tooth is attached to sustain function. Differences in cementum as a result of these functional characteristics would also be expected due to the different root configurations, distribution

NIH-PA Author Manuscript

NIH-PA Author Manuscript

NIH-PA Author Manuscript

of loads between teeth. Overall, the data collected elucidates the age-related changes within cementum and opens up the future prospect for an accurate age-related modeling of cementum and cementum dentin interfaces.

## Supplementary Material

Refer to Web version on PubMed Central for supplementary material.

## ACKNOWLEDGEMENTS

The authors acknowledge funding support NIH/NIDCR R00DE018212 (SPH), NIH/NIDCR R01DE022032 (SPH), NIH/NIDCR T32DE07306, and Departments of Preventive and Restorative Dental Sciences, UCSF. The authors also thank Prof. Lisa Pruitt for the use of the Hysitron Triboindenter, UC Berkeley, Prof. Peter Sargent for the use of the ultramicrotome, UCSF, and Joel Commisso of UC Davis (icpms.ucdavis.edu) for his help with ICP-MS.

## REFERENCES

1. Nanci, A. Ten Cate's oral histology : development, structure, and function. 7th ed.. St. Louis, MO: Mosby, Inc., and affiliate of Elsevier Inc.; 2007.
2. Bosshardt DD, Selvig KA. Dental cementum: the dynamic tissue covering of the root. Periodontol 2000. 1997; 13:41–75. [PubMed: 9567923]
3. Lin JD, Ozcoban H, Greene JP, Jang AT, Djomehri SI, Fahey KP, et al. Biomechanics of a bone-periodontal ligament-tooth fibrous joint. J Biomech. 2013; 46:443–449. [PubMed: 23219279]
4. Ho SP, Kurylo MP, Grandfield K, Hurng J, Herber RP, Ryder MI, et al. The plastic nature of the human bone-periodontal ligament-tooth fibrous joint. Bone. 2013; 57:455–467. [PubMed: 24063947]
5. Yamamoto T, Li M, Liu Z, Guo Y, Hasegawa T, Masuki H, et al. Histological review of the human cellular cementum with special reference to an alternating lamellar pattern. Odontology. 2010; 98:102–109. [PubMed: 20652787]
6. Ren LM, Wang WX, Takao Y, Chen ZX. Effects of cementum-dentine junction and cementum on the mechanical response of tooth supporting structure. J Dent. 2010
7. Rios HF, Ma D, Xie Y, Giannobile WV, Bonewald LF, Conway SJ, et al. Periostin is essential for the integrity and function of the periodontal ligament during occlusal loading in mice. J Periodontol. 2008; 79:1480–1490. [PubMed: 18672999]
8. Yamamoto T, Domon T, Takahashi S, Islam N, Suzuki R, Wakita M. The structure and function of periodontal ligament cells in acellular cementum in rat molars. Ann Anat. 1998; 180:519–522. [PubMed: 9862031]
9. Ho SP, Balooch M, Marshall SJ, Marshall GW. Local properties of a functionally graded interphase between cementum and dentin. Journal of biomedical materials research Part A. 2004; 70:480–489. [PubMed: 15293322]
10. Ho SP, Kurylo MP, Fong TK, Lee SS, Wagner HD, Ryder MI, et al. The biomechanical characteristics of the bone-periodontal ligament-cementum complex. Biomaterials. 2010; 31:6635–6646. [PubMed: 20541802]
11. Alvarez-Perez MA, Alvarez-Fregoso O, Ortiz-Lopez J, Arzate H. X-ray microanalysis of human cementum. Microsc Microanal. 2005; 11:313–318. [PubMed: 16079015]
12. Stamfelj I, Vidmar G, Cvetko E, Gaspersic D. Cementum thickness in multirooted human molars: a histometric study by light microscopy. Ann Anat. 2008; 190:129–139. [PubMed: 18413266]
13. Hopewell-Smith A. Concerning human cementum. J Dent Res. 1920:59–76.
14. Yamamoto T, Domon T, Takahashi S, Islam MN, Suzuki R. The fibrous structure of the cemento-dentinal junction in human molars shown by scanning electron microscopy combined with NaOH-maceration. J Periodontal Res. 2000; 35:59–64. [PubMed: 10863959]

NIH-PA Author Manuscript NIH-PA Author Manuscript NIH-PA Author Manuscript

15. Yamamoto T, Domon T, Takahashi S, Islam N, Suzuki R, Wakita M. The structure and function of the cemento-dentinal junction in human teeth. J Periodontal Res. 1999; 34:261–268. [PubMed: 10567949]
16. Yamamoto T, Domon T, Takahashi S, Islam N, Suzuki R. Twisted plywood structure of an alternating lamellar pattern in cellular cementum of human teeth. Anat Embryol (Berl). 2000; 202:25–30. [PubMed: 10926092]
17. Ho SP, Sulyanto RM, Marshall SJ, Marshall GW. The cementum-dentin junction also contains glycosaminoglycans and collagen fibrils. Journal of structural biology. 2005; 151:69–78. [PubMed: 15964205]
18. Parfitt AM. Age-related structural changes in trabecular and cortical bone: cellular mechanisms and biomechanical consequences. Calcif Tissue Int. 1984; 36(Suppl 1):S123–S128. [PubMed: 6430512]
19. Jubrias SA, Odderson IR, Esselman PC, Conley KE. Decline in isokinetic force with age: muscle cross-sectional area and specific force. Pflugers Arch. 1997; 434:246–253. [PubMed: 9178622]
20. Lexell J, Taylor CC, Sjostrom M. What is the cause of the ageing atrophy? Total number, size and proportion of different fiber types studied in whole vastus lateralis muscle from 15- to 83-year-old men. J Neurol Sci. 1988; 84:275–294. [PubMed: 3379447]
21. Hamrick MW, Ding KH, Pennington C, Chao YJ, Wu YD, Howard B, et al. Age-related loss of muscle mass and bone strength in mice is associated with a decline in physical activity and serum leptin. Bone. 2006; 39:845–853. [PubMed: 16750436]
22. Burr DB. Muscle strength, bone mass, and age-related bone loss. J Bone Miner Res. 1997; 12:1547–1551. [PubMed: 9333114]
23. Iinuma T, Arai Y, Fukumoto M, Takayama M, Abe Y, Asakura K, et al. Maximum occlusal force and physical performance in the oldest old: the Tokyo oldest old survey on total health. J Am Geriatr Soc. 2012; 60:68–76. [PubMed: 22211666]
24. Kiebzak GM. Age-related bone changes. Exp Gerontol. 1991; 26:171–187. [PubMed: 1915689]
25. Singh MA. Exercise comes of age: rationale and recommendations for a geriatric exercise prescription. J Gerontol A Biol Sci Med Sci. 2002; 57:M262–M282. [PubMed: 11983720]
26. Dalzell N, Kaptoge S, Morris N, Berthier A, Koller B, Braak L, et al. Bone micro-architecture and determinants of strength in the radius and tibia: age-related changes in a populationbased study of normal adults measured with high-resolution pQCT. Osteoporos Int. 2009; 20:1683–1694. [PubMed: 19152051]
27. Ikebe K, Nokubi T, Morii K, Kashiwagi J, Furuya M. Association of bite force with ageing and occlusal support in older adults. J Dent. 2005; 33:131–137. [PubMed: 15683894]
28. Hernandez CJ, Keaveny TM. A biomechanical perspective on bone quality. Bone. 2006; 39:1173–1181. [PubMed: 16876493]
29. Havill LM, Mahaney MC, T LB, Specker BL. Effects of genes, sex, age, and activity on BMC, bone size, and areal and volumetric BMD. J Bone Miner Res. 2007; 22:737–746. [PubMed: 17444815]
30. Mohr T, Podenphant J, Biering-Sorensen F, Galbo H, Thamsborg G, Kjaer M. Increased bone mineral density after prolonged electrically induced cycle training of paralyzed limbs in spinal cord injured man. Calcif Tissue Int. 1997; 61:22–25. [PubMed: 9192506]
31. Masoro, EJ.; Austad, SN. Handbook of the biology of aging. 5th ed.. San Diego, Calif.: Academic Press; 2001.
32. White JM, Goodis HE, Marshall SJ, Marshall GW. Sterilization of teeth by gamma radiation. J Dent Res. 1994; 73:1560–1567. [PubMed: 7929992]
33. Ho SP, Balooch M, Goodis HE, Marshall GW, Marshall SJ. Ultrastructure and nanomechanical properties of cementum dentin junction. Journal of biomedical materials research Part A. 2004; 68:343–351. [PubMed: 14704976]
34. Bei H, George EP, Hay JL, Pharr GM. Influence of indenter tip geometry on elastic deformation during nanoindentation. Phys Rev Lett. 2005; 95:045501. [PubMed: 16090818]
35. Wolf RL, Wehrli SL, Popescu AM, Woo JH, Song HK, Wright AC, et al. Mineral volume and morphology in carotid plaque specimens using high-resolution MRI and CT. Arterioscler Thromb Vasc Biol. 2005; 25:1729–1735. [PubMed: 15947239]

NIH-PA Author Manuscript

NIH-PA Author Manuscript

NIH-PA Author Manuscript


36. ASTM. E 384-99: Standard Test Method for Microindentation Hardness of Materials. West Conshohocken, PA: American Standard for Testing Materials International; 1999.
37. Jones SJ, Boyde A. Coronal cementogenesis in the horse. Arch Oral Biol. 1974; 19:605–614. [PubMed: 4532487]
38. Ho SP, Senkyrikova P, Marshall GW, Yun W, Wang Y, Karan K, et al. Structure, chemical composition and mechanical properties of coronal cementum in human deciduous molars. Dent Mater. 2009; 25:1195–1204. [PubMed: 19464049]
39. Listgarten M. Ultrastructure of the dento-gingival junction after gingivectomy. J Periodontal Res. 1972; 7:151–160. [PubMed: 4272041]
40. Silness J, Gustavsen F, Fejerskov O, Karring T, Loe H. Cellular, afibrillar coronal cementum in human teeth. J Periodontal Res. 1976; 11:331–338. [PubMed: 135828]
41. Sodek J, McKee MD. Molecular and cellular biology of alveolar bone. Periodontol 2000. 2000; 24:99–126. [PubMed: 11276877]
42. Saygin NE, Giannobile WV, Somerman MJ. Molecular and cell biology of cementum. Periodontol 2000. 2000; 24:73–98. [PubMed: 11276875]
43. Turner CH. Three rules for bone adaptation to mechanical stimuli. Bone. 1998; 23:399–407. [PubMed: 9823445]
44. Lanyon LE. Using functional loading to influence bone mass and architecture: objectives, mechanisms, and relationship with estrogen of the mechanically adaptive process in bone. Bone. 1996; 18:37S–43S. [PubMed: 8717546]
45. Melsen B, Lang NP. Biological reactions of alveolar bone to orthodontic loading of oral implants. Clin Oral Implants Res. 2001; 12:144–152. [PubMed: 11251664]
46. Roberts WE, Smith RK, Zilberman Y, Mozsary PG, Smith RS. Osseous adaptation to continuous loading of rigid endosseous implants. Am J Orthod. 1984; 86:95–111. [PubMed: 6589962]
47. Bakke M, Holm B, Jensen BL, Michler L, Moller E. Unilateral, isometric bite force in 8–68- year-old women and men related to occlusal factors. Scand J Dent Res. 1990; 98:149–158. [PubMed: 2343274]
48. Devlin H, Horner K, Ledgerton D. A comparison of maxillary and mandibular bone mineral densities. J Prosthet Dent. 1998; 79:323–327. [PubMed: 9553887]
49. Norton MR, Gamble C. Bone classification: an objective scale of bone density using the computerized tomography scan. Clin Oral Implants Res. 2001; 12:79–84. [PubMed: 11168274]
50. Nyman S, Lindhe J, Karring T, Rylander H. New attachment following surgical treatment of human periodontal disease. J Clin Periodontol. 1982; 9:290–296. [PubMed: 6964676]
51. Hughes FJ, Smales FC. Immunohistochemical investigation of the presence and distribution of cementum-associated lipopolysaccharides in periodontal disease. J Periodontal Res. 1986; 21:660–667. [PubMed: 2947999]
52. Toms SR, Dakin GJ, Lemons JE, Eberhardt AW. Quasi-linear viscoelastic behavior of the human periodontal ligament. J Biomech. 2002; 35:1411–1415. [PubMed: 12231287]
53. Smith RK, Roberts WE. Cell kinetics of the initial response to orthodontically induced osteogenesis in rat molar periodontal ligament. Calcif Tissue Int. 1980; 30:51–56. [PubMed: 6767534]
54. Zajicek G. Fibroblast cell kinetics in the periodontal ligament of the mouse. Cell Tissue Kinet. 1974; 7:479–492. [PubMed: 4422671]
55. Roberts WE, Jee WS. Cell kinetics of orthodontically-stimulated and non-stimulated periodontal ligament in the rat. Arch Oral Biol. 1974; 19:17–21. [PubMed: 4522924]
56. Norton, LA.; Burstone, C. The Biology of tooth movement. Boca Raton, Fla.: CRC Press; 1989.
57. Luan X, Ito Y, Holliday S, Walker C, Daniel J, Galang TM, et al. Extracellular matrixmediated tissue remodeling following axial movement of teeth. J Histochem Cytochem. 2007; 55:127–140. [PubMed: 17015623]
58. Selvig KA. The fine structure of human cementum. Acta Odontol Scand. 1965; 23:423–441. [PubMed: 5214199]
59. Lieberman DE. The Biological Basis for Seasonal Increments in Dental Cementum and Their Application to Archaeological Research. J Archaeol Sci. 1994; 21:525–539.

NIH-PA Author Manuscript

NIH-PA Author Manuscript

NIH-PA Author Manuscript

60. Kagayama M, Sasano Y, Mizoguchi I, Takahashi I. Confocal microscopy of cementocytes and their lacunae and canaliculi in rat molars. Anat Embryol. 1997; 195:491–496. [PubMed: 9193723]

61. Hatch JP, Shinkai RS, Sakai S, Rugh JD, Paunovich ED. Determinants of masticatory performance in dentate adults. Arch Oral Biol. 2001; 46:641–648. [PubMed: 11369319]

62. Kuhr A, Popa-Wagner A, Schmoll H, Schwahn C, Kocher T. Observations on experimental marginal periodontitis in rats. J Periodontal Res. 2004; 39:101–106. [PubMed: 15009517]

63. Niver EL, Leong N, Greene J, Curtis D, Ryder MI, Ho SP. Reduced functional loads alter the physical characteristics of the bone-periodontal ligament-cementum complex. J Periodontal Res. 2011; 46:730–741. [PubMed: 21848615]

64. Nakashima K, Zhou X, Kunkel G, Zhang Z, Deng JM, Behringer RR, et al. The novel zinc finger-containing transcription factor osterix is required for osteoblast differentiation and bone formation. Cell. 2002; 108:17–29. [PubMed: 11792318]

65. Brudevold F, Steadman LT, Spinelli MA, Amdur BH, Gron P. A study of zinc in human teeth. Arch Oral Biol. 1963; 8:135–144. [PubMed: 14016161]

66. Gilbert RJ, Ingram GS. The Oral Disposition of Zinc Following the Use of an Anticalculus Toothpaste Containing 0.5-Percent Zinc Citrate. J Pharm Pharmacol. 1988; 40:399–402. [PubMed: 2901470]

67. Yamaguchi M, Oishi H, Suketa Y. Zinc stimulation of bone protein synthesis in tissue culture. Activation of aminoacyl-tRNA synthetase. Biochem Pharmacol. 1988; 37:4075–4080. [PubMed: 2461201]

68. Hohmann A, Wolfram U, Geiger M, Boryor A, Kober C, Sander C, et al. Correspondences of hydrostatic pressure in periodontal ligament with regions of root resorption: a clinical and a finite element study of the same human teeth. Comput Methods Programs Biomed. 2009; 93:155–161. [PubMed: 18951647]

NIH-PA Author Manuscript

NIH-PA Author Manuscript

NIH-PA Author Manuscript

## Highlights

- Physical and chemical properties of primary and secondary cementum types changed with age.
- Observed changes were indicative of adaptation of cementum appositional layers with age.
- Physicochemical changes were also observed in the hygroscopic cementum dentin interface.

NIH-PA Author Manuscript

NIH-PA Author Manuscript

NIH-PA Author Manuscript

a

| Specimen Age (years) | Younger | Middle | Older |
|---|---|---|---|
| Age Range | 19-39 | 40-60 | 61-81 |
| Microindentation, Nanoindentation, & Microscopy | 23±5.1 (N=6) | 48±8.8 (N=4) | 74±8.0 (N=4) |
| ICP-MS | 27±9.5 (N=9) | 49±6.2 (N=8) | 66±1.7 (N=12) |

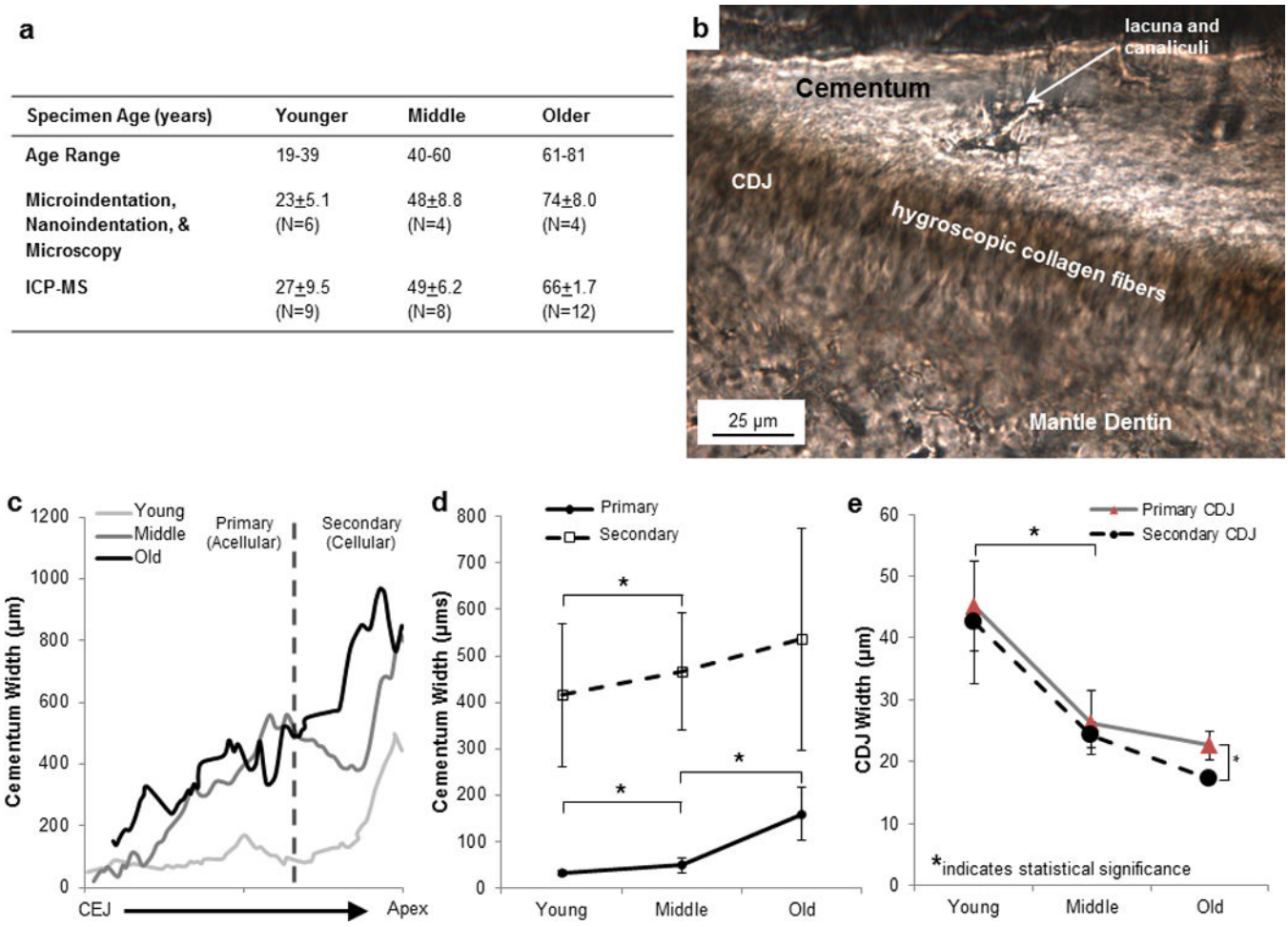


**Figure 1.**

(a) Age ranges of younger, middle, and older humans from whom teeth obtained were used for microscopy (second row; mean +/− standard deviation), microindentation, nanoindentation, and inductively coupled plasma mass spectroscopy (ICP-MS) (third row; mean +/− standard deviation). Sample size of each group is shown in parentheses. (b) Transmission light microscopy images of sectioned molars demonstrate the clear fibrous cementum-dentin junction (CDJ). (c) Representative graphs of cementum width vs. anatomical location show a two-step increase in cementum thickness when measured from the cementum enamel junction (CEJ) to the root apex regions, that is, along the length of the root. (d) Graph of average cementum width across age groups for primary cementum (PC) and secondary cementum (SC) regions. In general, SC was thicker than PC and cementum thickness generally increased as a function of age. Statistical significant ($p<0.05$) relationships are indicated with an asterisk (*). (e) The thickness of the collagenous band indicative of the CDJ within the PC and SC regions decreased with age. Additionally, a decrease in apical CDJ width compared to the coronal CDJ in younger group was observed. However the CDJ width for middle and older groups was not different.

NIH-PA Author Manuscript
NIH-PA Author Manuscript
NIH-PA Author Manuscript



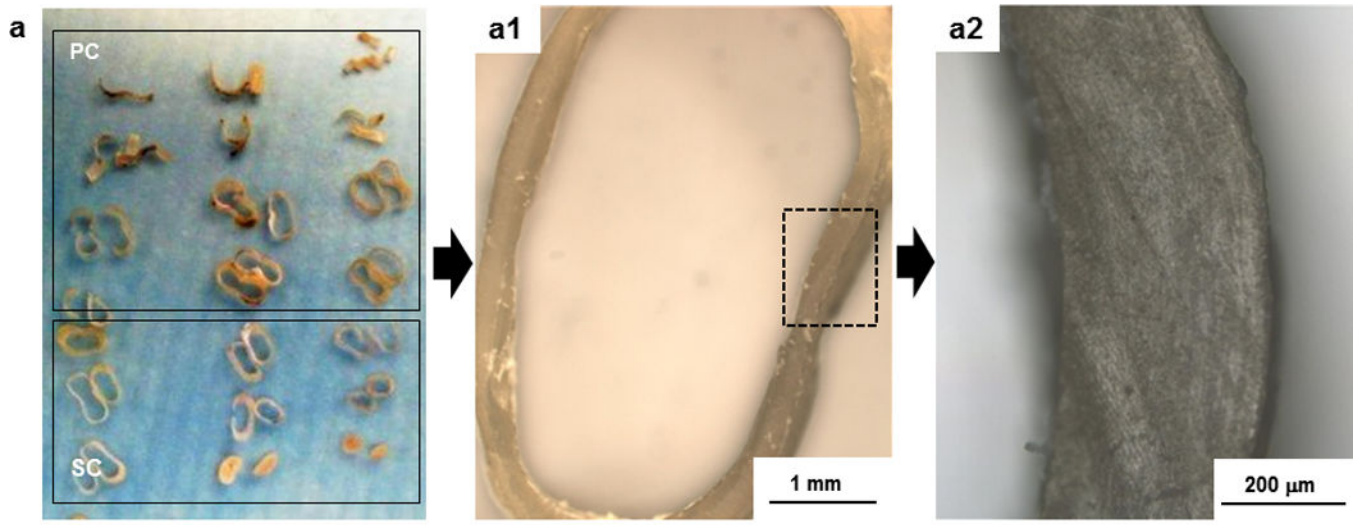


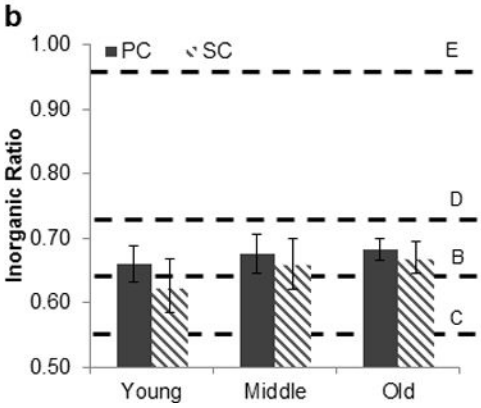


c

| Location | Element wt. % (SD) | NIST 1400 Bone Ash | Younger (19-39 yrs) | Middle (40-60 yrs) | Older (61-81 yrs) |
|---|---|---|---|---|---|
| PC | % Inorganic | | 0.66 (0.03) | 0.67 (0.03) | 0.68 (0.02) |
| | Calcium | 38.1 (0.13) | 56 (9.6) | 56 (4.9) | 54 (12) |
| | Magnesium | 0.68 (0.01) | 0.92 (0.23) | 0.87 (0.09) | 0.85 (0.11) |
| | Zinc | 0.181 (0.003) | 0.04 (0.02) | 0.04 (0.01) | 0.04 (0.02) |
| SC | % Inorganic | | 0.63 (0.04) | 0.66 (0.04) | 0.67 (0.02) |
| | Calcium | | 63.0 (6.5) | 65.0 (5.0) | 53 (19) |
| | Magnesium | | 0.91 (0.13) | 0.88 (0.33) | 0.73 (0.23) |
| | Zinc | | 0.06 (0.01) | 0.06 (0.01) | 0.06 (0.06) |

**Figure 2.**

(a) Isolated cementum rings for ICP-MS analysis were sorted by anatomical location and tooth specimen (PC – primary cementum, SC – secondary cementum). Confirmation of dentin removal was performed by checking for any remnant dentin by using a light microscope for all specimens as shown at several magnification (a1 and a2). (b) Graph highlights inorganic ratio (ash weight/preburn weight) of cementum as measured in this study vs. age relative to reported values (dashed lines) for mineralized tissues enamel (E), dentin (D), and alveolar bone (B), including cementum (C) [1]. (c) A table of inorganic ratio and percentage of elemental composition (by weight) for calcium, magnesium, and zinc is shown for all age groups in primary and secondary cementum (PC, SC) types. The elemental standard (NIST 1400-bone ash) used for analysis is also included.

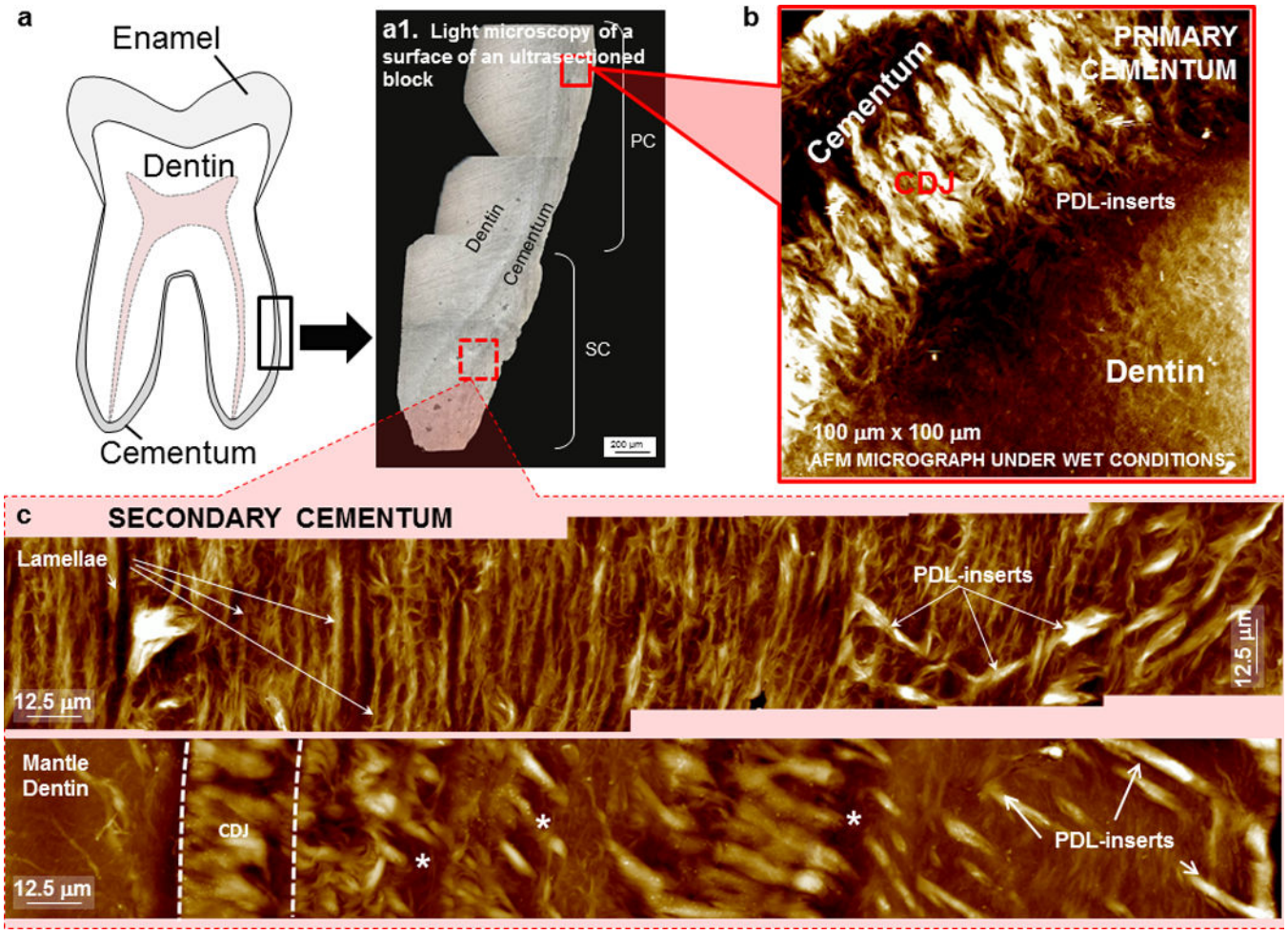


**Figure 3.**

(a) Schematic of a tooth highlighting a region (rectangle) that was ultrasectioned for imaging using light (a1) and atomic force microscopy techniques (b, c). The surface of the ultrasectioned block contains regions that were imaged using an AFM (red squares with solid and dashed lines). AFM micrographs illustrate fibrous CDJ region in primary cementum (b) and in secondary cementum (c) under hydrated conditions. (c) The structure of secondary cementum includes lamellae, PDL-inserts (arrows), and the CDJ (the zone between the dashed lines). Incremental lines indicating growth are shown asterisk (*) with about a 10 – 40 µm spacing between each line.



NIH-PA Author Manuscript NIH-PA Author Manuscript NIH-PA Author Manuscript

NIH-PA Author Manuscript
NIH-PA Author Manuscript
NIH-PA Author Manuscript



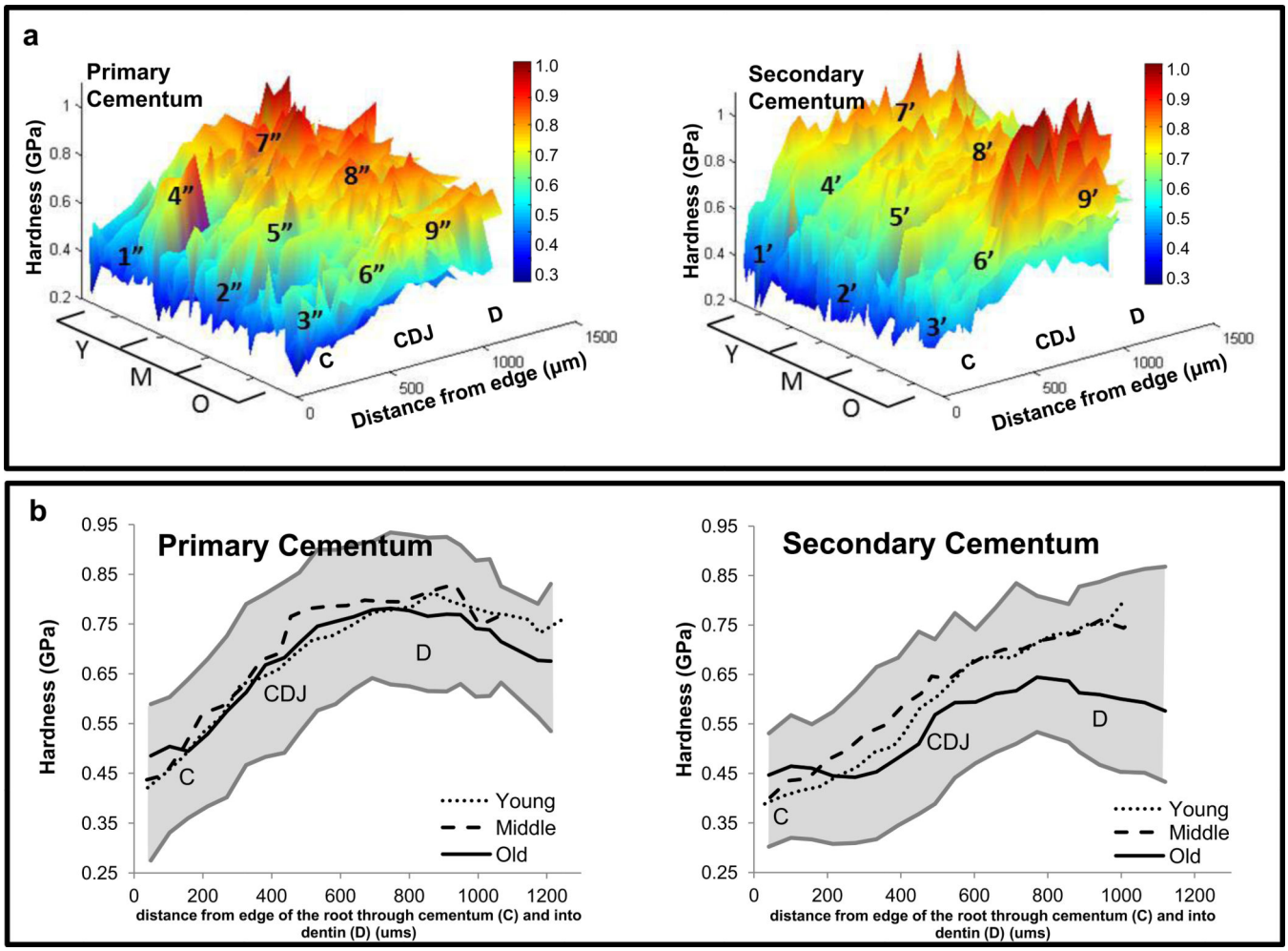


**Figure 4.**

Knoop hardness variations were grouped by age and location (from edge of the root through cementum (C) and into dentin (D)). (a) Hardness data from microindentation was graphed against age (Y: younger, M: middle, O: older) and from the cementum enthesis (edge of the root where the periodontal ligament meets cementum to dentin in order to depict the increase in hardness with age. Note that 1” – 9” represent hardness values for PC, CDJ, D, and 1’–9’ represent hardness values for SC, corresponding CDJ, and D. (b) Averages for each age and general trends were calculated to illustrate a gradual shift in material hardness between cementum and dentin. Grey zones represent 95% upper and lower bounds for all age groups.

NIH-PA Author Manuscript

NIH-PA Author Manuscript

NIH-PA Author Manuscript

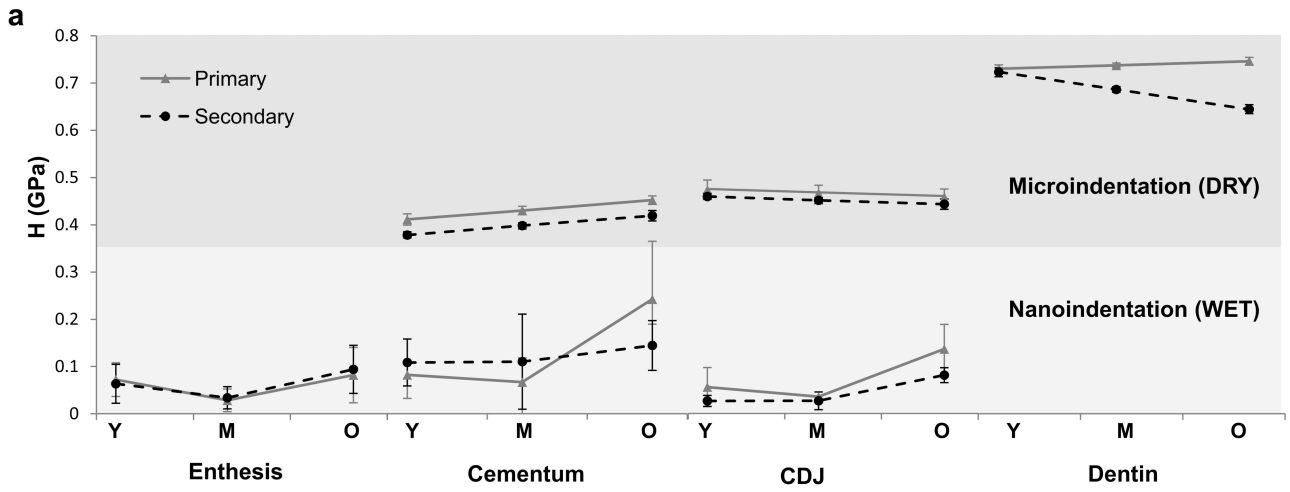


| b | | Young – H (GPa) | | | | Middle – H (GPa) | | | | Old – H (GPa) | | | |
|---|---|---|---|---|---|---|---|---|---|---|---|---|---|
| | | PDL-C (En) | C | CDJ | D | PDL-C (En) | C | CDJ | D | PDL-C (En) | C | CDJ | D |
| Micro (Dry) | 1° | | 0.41(0.01) | 0.48(0.02) | 0.73(0.01) | | 0.43(0.01) | 0.47(0.02) | 0.74(0.01) | | 0.45(0.01) | 0.46(0.02) | 0.75(0.01) |
| | 2° | | 0.38(0.01) | 0.46(0.02) | 0.72(0.01) | | 0.40(0.01) | 0.45(0.01) | 0.69(0.01) | | 0.42(0.01) | 0.44(0.01) | 0.64(0.01) |
| Nano (Wet) | 1° | 0.07(0.04) | 0.08(0.03) | 0.06(0.04) | | 0.03(0.02) | 0.07(0.05) | 0.04(0.01) | | 0.08(0.06) | 0.24(0.12) | 0.14(0.05) | |
| | 2° | 0.06(0.04) | 0.11(0.05) | 0.03(0.01) | | 0.03(0.02) | 0.11(0.10) | 0.03(0.02) | | 0.09(0.05) | 0.14(0.05) | 0.08(0.02) | |

**Figure 5.**

Plotted graphs (a) and table values (b, averages (standard deviations)) illustrate hardness values across the enthesis (En, PDL-cementum interface), cementum (C), cementum dentin junction (CDJ), and dentin (D). (b) shows an increasing trend in hardness as a function of age. Incremental changes in hardness between regions illustrate a mechanical continuum across these tissues. Notice that both cementum and dentin show similar age related trends in the apical and coronal regions while dentin exhibits an age and location interaction effect. 1°: Primary Cementum, 2°: Secondary Cementum.